

GEOMECHANICAL ANALYSIS OF SEDIMENTARY LAYERING AS A STRUCTURAL CONTROL ON FAULT PROPAGATION

CURTIS SEGARRA, Trinity University
Research Advisor: Dr. Benjamin Surples

INTRODUCTION

Deformation associated with normal fault propagation and displacement places controls on the distribution and flow of sub-surface fluids. With a better understanding of how sedimentary units deform in response to a propagating fault, scientists can better predict how fluids might flow through the system at different stages of displacement. Though previous researchers have acknowledged the effects of sedimentary layering as barriers to fault propagation (e.g. Cooke and Pollard, 1997; Cooke et al., 2001; Peacock, 2002; Hayano and Ishii, 2016), previous research has failed to produce a systematic, quantitative analysis of the role of mechanical layering on fault tip propagation. Therefore, building upon previous geomechanical modeling techniques (Smart et al., 2004, 2009, 2010b, 2010a, 2012; Doff, 2015; Sattari and Eaton, 2015), I use ABAQUS/Standard finite element modeling software (by Dassault Systemes, 2018) to create an experimental finite element model that permits me to analyze the influence of stratigraphic layering upon stress and strain ahead of a fault tip.

I use finite element analysis (FEA), a method for calculating a specific output quantity, such as stress or strain, as a solution to a defined mathematical problem, within a complex, multi-piece model (Cook, 1995). By dividing a model into “elements”, across which displacement, stress, and strain can be interpolated, I analyze the spatial distribution of stress and strain fields (Cook, 1995). I use this technique to addresses two research goals: 1. To systematically analyze the influence of planar bedding upon stress and strain fields ahead of a propagating normal fault;

and 2. To develop a predictive model of fracture distribution during propagation of a normal fault through bedded stratigraphy. This approach permits me to control the most important physical variables (e.g., bedding thickness, fault displacement, material properties of rock layers), and the software permits me to efficiently model changes in different factors (e.g., coefficient of friction between beds, number of beds) across a range of values.

METHODOLOGY

Model Development

My model replicates a 60°-dipping, planar, dip-slip normal fault, a geometry that represents normal fault systems at depths shallower than 10 km (Jackson and McKenzie, 1983). My model captures initial stages of propagation of a pre-existing fault into undeformed sandstone beds with thicknesses on the several-meter scale range; I do not examine initial fault formation, but instead, I focus my modeling efforts on initial stages of propagation through layered strata.

I use a model geometry similar to the geometry used by Smart et al. (2010a). The underlying fault block of the footwall (B1, Fig. 1) imposes displacement on the model. The overlying fault block of the footwall (B3, Fig. 1), provides an overburden load and is not restrained. Pinned fault blocks in the hanging wall (B2 and B3, Fig. 1) cannot move horizontally nor vertically, ensuring displacement occurs along the fault plane.

The mesh density, as defined by the size of “elements,” which each model piece is divided into for mathematical interpolation of stress and strain,

controls the permissible deformation of each model piece and the resolution of the results. Because I do not intend to deform the four bounding blocks of the model (B1 through B4), I define a coarse mesh for the four bounding blocks. Mesh resolution of the test beds is fine near the center of the beds and coarse near the edges of the model, ensuring higher-resolution analysis near the propagating fault. The vertical mesh resolution is constant; each element is 1 meter tall. Since the four fault blocks surrounding the test beds do not deform, the mesh resolution does not affect the results; coarser mesh in the fault blocks aids computational efficiency.

Following Smart et al.'s (2010a) modeling protocol, I employ elastic-plastic material behavior for the deformable beds and an elastic material with a high Young's Modulus (30 GPa) for the fault blocks (B1 through B4, Fig. 1); the material properties (Table 1) are held constant throughout each model.

Within my model, I define the fault surface and orientation as a planar, non-frictional contact. Similarly, I define contacts between the test beds and the fault blocks as planar, non-frictional contacts. I do not analyze the role of these outer contacts. The contacts between test strata (T1-T3, Fig. 1) are frictional planar contacts; I vary the coefficient of friction between test beds from 0.15 μ to 0.9 μ .

Within test strata, I prescribe a pre-existing internal stress state for all elements (stress tensor, Fig. 1); I pair this stress with inward forces applied to the top and sides of the model (Fig. 1), which simulate stresses due to a small overburden. There are no pre-existing weaknesses in the undeformed test beds.

Analysis

In the modeling presented here, I perform a three-step analysis. In the initial step, I apply boundary conditions. In the second step, I apply forces to the model, allowing the model to achieve equilibrium and begin displacement. Total displacement is incremented non-uniformly based upon the computational complexity of the model. Finally, once the displacement is complete, I review the results in the output step. I apply this procedure to one 20-meter-thick bed, two 10-meter-thick beds, three 6.67-meter-

thick beds, four 5-meter-thick beds, and five 4-meter-thick beds, which permits me to analyze the influence of planar bedding upon the stress and strain fields within the beds. Additionally, I vary the coefficient of friction between the beds, which permits me to assess the influence of inter-layer friction upon stress and strain field development.

RESULTS

Initial Plastic Failure

For each iteration of the model, initial plastic failure occurred at displacements between 0.030 meters and 0.040 meters and was spatially localized. Some models failed at only one region, others at two regions (Fig. 2), with failure restricted to the lowermost and uppermost layers of the test package (Fig. 2). This means that, where simultaneous initial failure occurred, initial plastic failure occurred close to the propagating fault tip (1-4 meters from the fault tip) as well as up to 19 meters from the propagating tip. The distribution of simultaneous initial failure, where three or more beds were deformed, is symmetrical about the center of the test strata (Fig. 2)

Stress Distribution

At displacements causing initial plastic failure, in-plane principal stress is highest in the uppermost and lowermost mechanical layers, reaching values of over 10 MPa (Fig. 2). Within a single layer, in-plane principal stress is highest in the base of the hanging wall of the test layer (Fig. 2). Additionally, the model with no layering exhibits a smooth gradient of stress

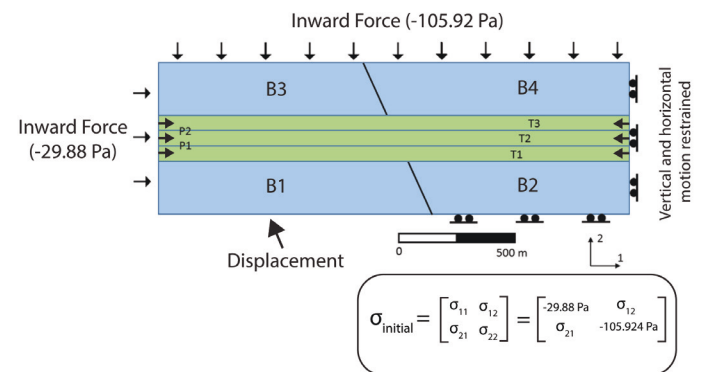


Figure 1. Example of model geometry and forces. This example shows three test beds (T1-T3).

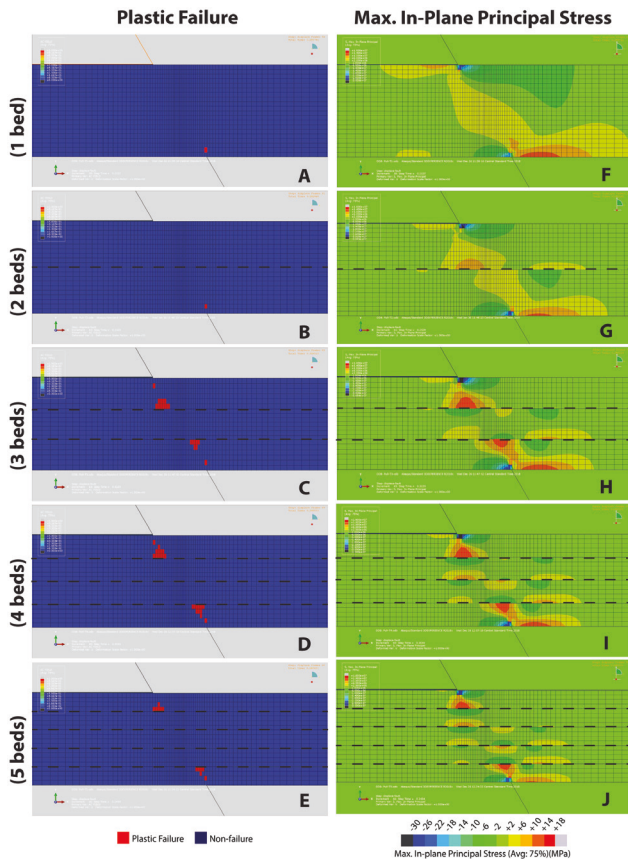


Figure 2. Initial plastic failure (A-E) and stress gradients (F-J) at low levels of displacement, with constant friction between layers (0.15μ). Dashed line indicates bedding plane. Note the presence of three or more beds (C-E) results in multiple locations of simultaneous plastic failure. Note that initial failure is confined to the lowermost and uppermost mechanical layers in each model (A-E). Note that mechanical layering (G) through (J) distorts the smooth gradient seen when no layering is present (F). Note how increasing mechanical layering allows for higher stress concentrations near the center of the test strata (G-J).

ahead of the propagating fault tip (Fig. 2). When mechanical layering is present, this smooth in-plane gradient becomes discontinuous, strongly affected by boundaries between mechanical layers (Fig. 2). In addition, in-plane principal stress near the center of the multi-bed package of test strata (in the center of the model) is elevated relative to the level of stress in the center of the single bed model. Although not explored in detail here, increased friction between mechanical layers results in the development of a more continuous gradient of in-plane principal stress from one mechanical boundary to the next (model not shown).

Strain Development

When only one mechanical layer is deformed in the

model, increased displacement leads to a smooth, along-fault-plane accumulation of in-plane principal strain. At displacement levels causing initial plastic failure, the presence of mechanical layering discretizes strain at the mechanical boundaries (Fig. 3). In every model with mechanical layering, logarithmic in-plane principal strain is maximized in the uppermost and lowermost mechanical layers (similarly indicated by the location of initial plastic failure) (Fig. 3).

Through-going Failure and Stress Distribution

With continued displacement (0.07 to 0.09 m), through-going plastic failure occurred throughout the entire 20 m test section (Fig. 4). This increased displacement caused stress gradients ahead of the propagating fault tips to become less discontinuous than in the earliest stages of propagation (Fig. 4). By the time through-going failure occurred, stress was relatively concentrated along the plane of the propagating fault, but off-fault-plane distributions of stress do occur. With increasing friction between layers, stresses are distributed further from the fault plane (model not shown).

DISCUSSION

I used 2D finite element modeling to assess the role of mechanical layering in the initial stages of normal fault tip propagation. By varying the number of mechanical layers present (one layer to five layers), I found that the presence of layers inhibits the development of a smooth stress gradient ahead of the propagating fault tip. This leads to simultaneous, discontinuous plastic failure at multiple locations ahead of the fault tip during the initial stages of propagation. With the material properties defined to represent a 20 m thick test section of sandstone, I find that a displacement of 0.03 to 0.04 meters is sufficient to cause plastic failure.

With continued displacement (0.07 to 0.09 m), through-going plastic failure occurred throughout the entire 20 m test section. This increased displacement caused stress gradients ahead of the propagating fault tips to become more continuous than in the earliest stages of propagation. As such, by the time through-going failure occurred, stress was primarily

Max. Log. In-Plane Principle Strain

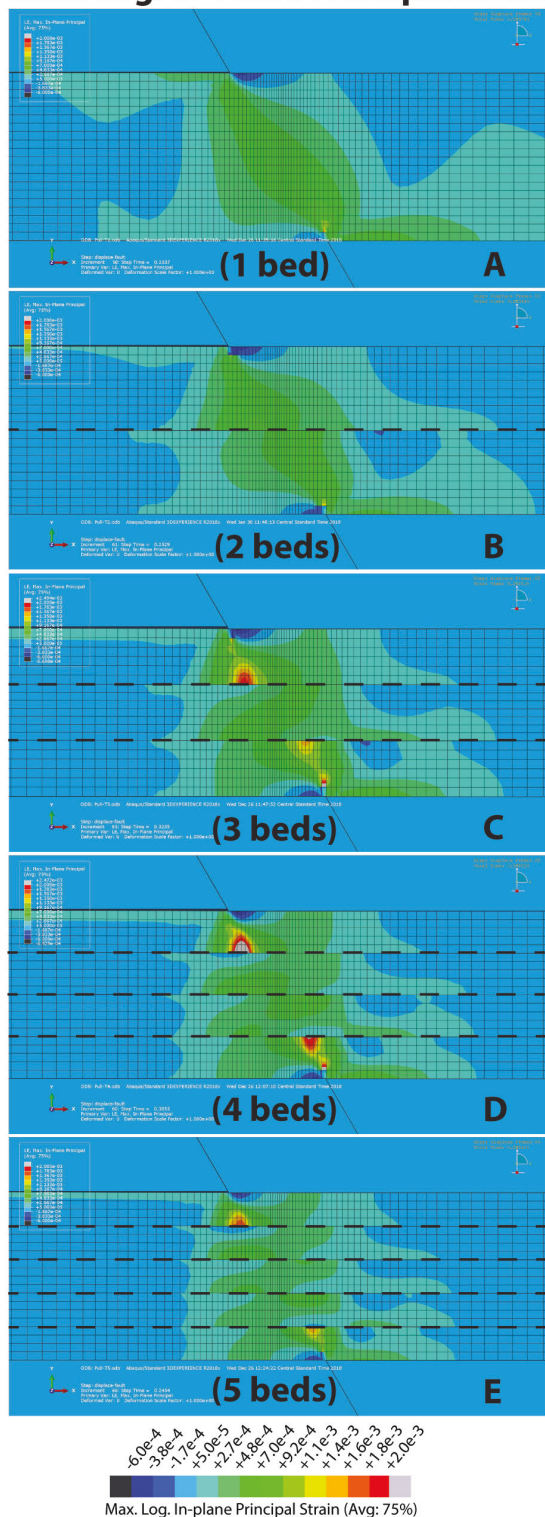


Figure 3. Maximum logarithmic in-plane principal strain gradients at low levels of displacement, with constant friction between layers (0.15μ). (A) No mechanical layering, (B) two layers, (C) three layers, (D) four layers, (E) five layers. Dashed line indicates bedding plane. Note that mechanical layering (B) through (E) distorts the smooth gradient seen when no layering is present (A). Note how increasing mechanical layering allows for strain accumulation in the uppermost and lowermost layers.

concentrated in-plane with the propagating fault.

I find that varying the coefficient of friction of the contacts between mechanical layers has minimal effect on the development of plastic failure; however, varying friction does affect the distribution of stress within the test strata. Increasing friction leads to a smoother stress gradient and minimizes the discontinuous localization of strain at mechanical layer boundaries.

At all levels of displacement, stress tends to accumulate in the hanging wall, out of plane from the fault. Under 0.07 m to 0.09 m displacement, increasing friction causes this accumulation of stress in the hanging wall to occur further from the fault plane.

My models suggest that the initial stages of fault tip propagation of a normal fault within a layered system are not characterized by linear stress gradients leading to in-plane plastic failure. Rather, the initial stages of propagation are characterized by complex patterns of stress accumulation. The presence of discontinuous regions of increased stress along layer boundaries leads to simultaneous plastic failure at multiple locations ahead of the propagating fault tip. This suggests that under low levels of displacement, a layered system is more likely to produce multiple, discontinuous fracture regions than in a single-layer system. Within a field setting, I would expect fracturing and potential fluid conduits to develop where the plane of a propagating fault tip intersects bedding planes. Additionally, my modeling suggests regions of increased stress off-plane from the propagating fault tip. In my model, these stress accumulations occurred in the hanging wall, but I would expect differing boundary conditions to lead to similar accumulations in the footwall. My results suggest that fracturing would be likely to occur away from the projected fault plane, localized along bedding plane boundaries.

As one of the first attempts to model the influence of planar bedding upon the stress and strain fields ahead of a propagating normal fault, my findings should be considered preliminary. However, these results reveal the power of finite element analysis to predict

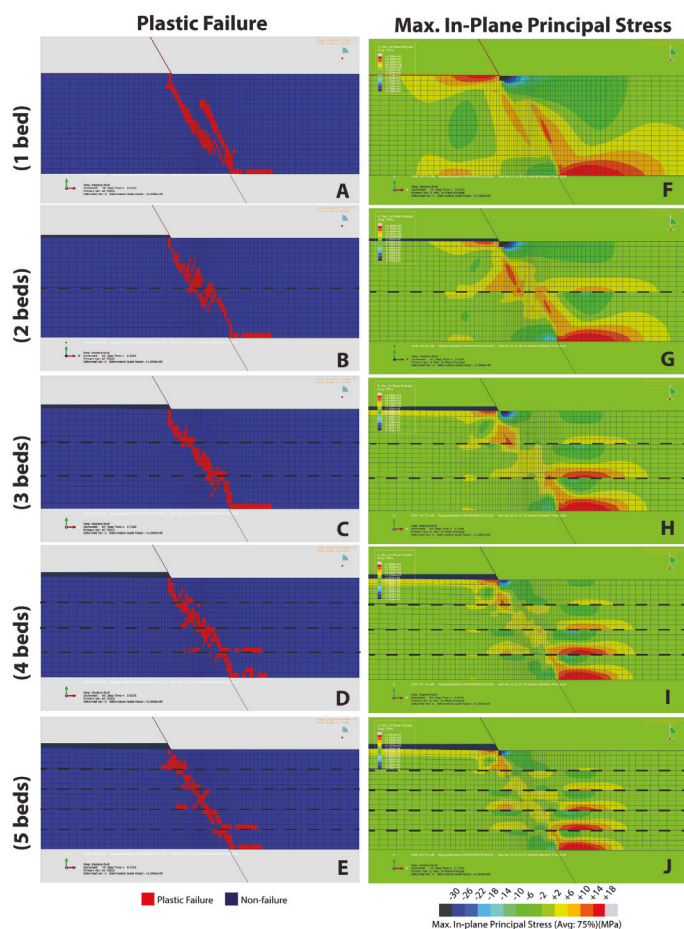


Figure 4. Initial plastic failure (A-E) and stress gradients (F-J) and at levels of displacement that cause through-going plastic failure, with constant friction between layers (0.15μ). Dashed line indicates bedding plane. Note the presence of four or more beds (D & E) results in plastic failure along multiple bedding planes. Note that failure accumulates where the hanging wall contacts the grey fault block (A-E). Note that mechanical layering (G-J) distorts the smooth stress gradient seen when no layering is present (F). Note how increasing mechanical layering allows for increased stress concentrations off-plane from the fault, in the hanging wall (F-J).

the distribution of fracture initiation relative to a fault propagating through bedding. Thus, an FEA approach may aid in subsurface resource conduit exploration and for modeling stress and strain fields near faults.

ACKNOWLEDGEMENTS

This material is based upon work supported by the Keck Geology Consortium and the National Science Foundation under Grant No. 1659322. Additionally, my research was funded, in-part, by the Trinity University Geosciences Department. Finally, I would like to thank Dr. Kevin Smart at SWRI for showing me how to use ABAQUS effectively.

REFERENCES

- Cook, R.D., 1995, Finite element modelling for stress analysis: John Wiley & Sons, Inc.
- Cooke, M.L., and Pollard, D.D., 1997, Bedding-plane slip in initial stages of fault-related folding: *Journal of Structural Geology*, v. 19, no. 3-4, p. 567-581.
- Cooke ML, and Underwood, C.A., 2001. Fracture termination and step-over at bedding interfaces due to frictional slip and interface opening, *Journal of Structural Geology*, 23: 223–238.
- Dassault Systèmes, 2018, ABAQUS/Standard 3DEXPERIENCE [Computer Software].
- Doff, J., 2015, Geomechanical modelling of a fault-propagation fold [bachelor's thesis]: TUDelft, 2015.
- Hayano, A., and Ishii, E., 2016, Relationship between faults oriented parallel and oblique to bedding in Neogene massive siliceous mudstones at the Horonobe Underground Research Laboratory, Japan: *IOP Conf. Ser.: Earth Environ. Sci.*, v. 44.
- Jackson, J., and McKenzie, D., 1983, The geometrical evolution of normal fault systems: *Journal of Structural Geology*, v. 5, p. 471-482.
- Peacock, D.C.P., 2002, Propagation, interaction and linkage in normal fault systems: *Earth-Science Reviews*, v. 58, p. 121-142.
- Sattari, A., and Eaton, D.W., 2015, 3D finite element modelling of fault-slip triggering caused by pore-pressure changes in GeoConvention 2015: New Horizons, Calgary, Canada.
- Smart, K.J., Ferrill, D.A., Sims, D.W., Franklin, N.M., Ofoegbu, G.I., Morris, A.P., 2004, Integrated structural analysis and geomechanical modelling: an aid to reservoir exploration and development: *Gulf Rocks 2004 – 6th North American Rock Mechanics Symposium: Rock Mechanics Across Borders & Disciplines*. Houston, TX, 5–9 June 2004: ARMA/NARMS Paper 04–470.

- Smart, K.J., Ferrill, D.A., and Morris, A.P., 2009, Impact of interlayer slip on fracture prediction from geomechanical models of fault-related folds: American Association of Petroleum Geologists Bulletin 93, 1447–1458.
- Smart, K.J., Ferrill, D.A., Morris, A.P., Bichon, B.J., Riha, D.S., and Huyse, L., 2010a, Geomechanical modelling of an extensional fault-propagation fold: Big Brushy Canyon monocline, Sierra Del Carmen, Texas: American Association of Petroleum Geologists Bulletin 94, 221–240.
- Smart, K.J., Ferrill, D.A., Morris, A.P., and McGinnis, R.N., 2010b, Geomechanical modelling of a reservoir-scale fault-related fold: the Bargy anticline, France: 44th U.S. Rock Mechanics Symposium, ARMA Paper 10–201.
- Smart, K.J., Ferrill, D.A., Morris, A.P., and McGinnis, R.N., 2012, Geomechanical modelling of stress and strain evolution during contractional fault-related folding: Tectonophysics, v. 576-577, p. 171-196.
- Smart, K.J., 2018, personal communication.